



SHAPE OPTIMIZATION OF BUTTERFLY-SHAPED SHEAR LINKS USING GREY WOLF ALGORITHM

Alireza Farzampour¹, Mohsen Khatibinia², Iman Mansouri³

¹Department of Civil and Environmental Engineering, Virginia Tech, United States

²Department of Civil Engineering, University of Birjand, Birjand, Iran

³Department of Civil Engineering, Birjand University of Technology, P.O. Box 97175-569,
Birjand, Iran

SUMMARY: *The shear loading applied to structures is resisted by implementation of hysteretic dampers as structural seismic force resisting system. Recently, steel plates with engineered cut-outs are introduced to have controlled yielding. These structural elements behave as shear links are able to postpone brittle limit states, leading to resistance against early fracture. Among which, a promising type of link is butterfly-shaped link, for which the demand moment diagram aligns with capacity moment diagram to efficiently implement the steel. Previous studies show that these elements are used as appropriate choice for structural seismic fuse system since they are able to experience large drifts with sufficient ductility and full hysteretic behavior. Therefore, the appropriate geometrical properties for these links are in need of further investigations. In this study, the finite element methodology is initially validated with experimental test. Then optimization criteria is introduced for set of 300 models to investigate the desired geometrical properties for having most energy dissipation with less fracture potential. This paper represents optimization process with which the geometrical properties of butterfly shaped link is improved to have sufficient energy dissipation performance and less potential for fracture. The pushover curves and equivalent plastic strains are obtained from ABAQUS through an iterative process. The Grey Wolf Optimizer method is adopted for optimization methodology due to having strong capability in non-linear system. It can be found that by implementation of optimization methodology the links are designed to have a mode switch from flexural yielding limit state to shear yielding and are able to dissipate energy over a less equivalent plastic strain value.*

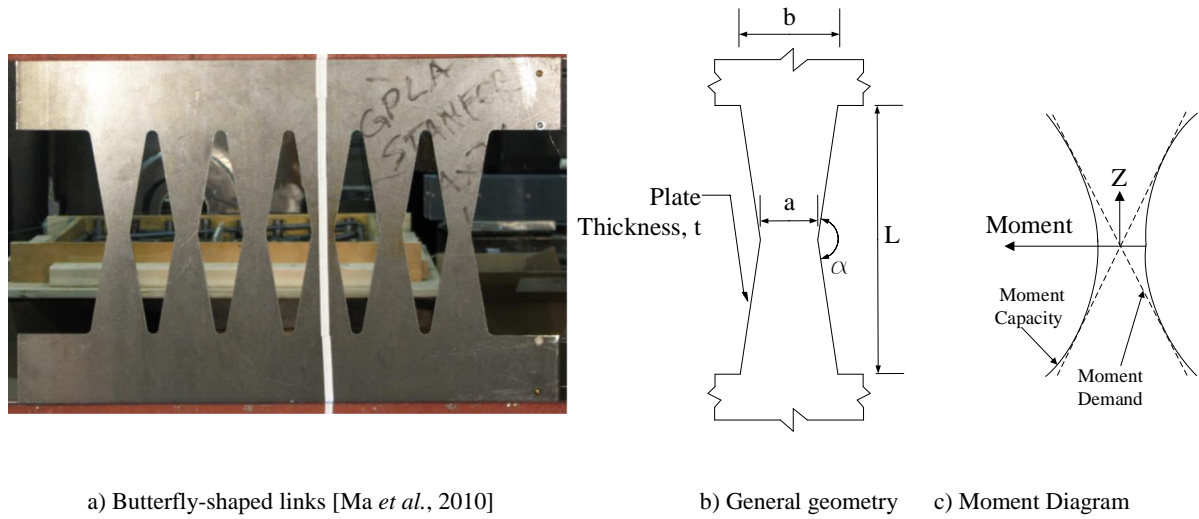
KEYWORDS: Structural Seismic fuses, Grey wolf optimization, Butterfly-shaped links, Finite element, Plastic strain

1 Introduction

Structural fuses are implemented within the structures to protect the surrounding members from damages and concentration of inelasticity in a specific area [Lee *et al.*, 2015a, Lee *et al.*, 2016a, Lee *et al.*, 2016b, Lee *et al.*, 2015b, Longo *et al.*, 2016, Mirzai *et al.*, 2018, Montuori *et al.*, 2016, 2017a, Montuori *et al.*, 2017b, Nastri *et al.*, 2015]. These fuses behave as steel plates subjected to shear loading which increase the energy dissipation capability against cyclic loading conditions [Castaldo *et al.*, 2016, Zeynali *et al.*, 2018]. Previous works showed that structural fuses are capable of providing elastic stiffness, ductility and energy dissipation capability [Farzampour, 2019, Farzampour and Eatherton, 2018a, 2018b, Farzampour and Eatherton, 2019, Hitaka and Matsui, 2003, Martínez-Rueda, 2002, Teruna *et al.*, 2015]. One

class of structural fuses are constructed in steel plates with links cut into them. These links, if appropriately designed [Farzampour and Eatherton, 2017] would be able to yield and resist the lateral forces when the plate is subjected to shear, which leads to sufficient damping of the imposed energy and decreasing the demand forces on the rest of the structural elements.

In order to better align the bending moment capacity diagrams with the corresponding demand diagram along the length of the links, Butterfly-Shaped Links (BSLs) with varying width between larger ends and a smaller middle section are proposed. These links, shown in Figure 1, are capable of substantial ductility, and load bearing capability without strength and stiffness degradation [Farzampour and Eatherton, 2018b, Ma *et al.*, 2010]. The planar geometry of the butterfly-shaped links with buckling resistance capability, make them a preferable seismic resistance system for space-constrained areas in structures as well.

a) Butterfly-shaped links [Ma *et al.*, 2010]

b) General geometry

c) Moment Diagram

Figure 1 - *The butterfly-shaped hysteretic damper*

Traditionally, added damping and stiffness hysteretic dampers (ADAS), and triangular-plate added damping and stiffness device (TADAS) are tested to resist the lateral loading by bending about the minor axis [Whittaker *et al.*, 1991]. However, the implementation of the in-plane format of butterfly-shaped links could be useful as the initial stiffness, distribution of yielding stresses over the length of the links are improved by significant margin [Farzampour and Eatherton, 2017, 2018a, 2018b]. Potential advantages of the BSLs are that these fuses require less operation for construction and the flat shape makes them suitable for a numerous structural system. The butterfly-shaped links when subjected to shear loading, could develop controlled flexural yielding. There are a few number of studies on improving the behavior of the BSLs, to control the location of yielding [Farzampour and Eatherton, 2017], delaying the fracture and increasing the energy dissipation capabilities. Due to the dearth of knowledge and increasing the demand of implementation of BSLs in various applications and systems [Luth *et al.*, 2008], there is a need to optimize these fuses with currently soft computation methodologies to improve the design methodologies and structural performance of these structural seismic fuses. In this study, the finite element simulation methodology is validated with the well-established experimental tests. Over the last decade, many researchers have employed the optimization algorithms in several applications in structural engineering [Deng *et al.*, 2014, Jiménez-Alonso and Sáez, 2017, Khatibinia and Sadegh Naseralavi, 2014, Liu *et al.*, 2016, Mansouri *et al.*,

2016, Mirzai *et al.*, 2017, Mukhopadhyay *et al.*, 2015, Okasha, 2016, Salajegheh *et al.*, 2008, Zhu *et al.*, 2018]. In this paper, a set of 300 models are considered to optimize the general geometrical properties of the BSLs. Grey Wolf Optimizer (GWO) is implemented to generate the optimization function based on the energy dissipation capability and concentration of plastic strain within each model. A total of 300 models are generated with finite element software and then optimized accordingly. The optimized values for butterfly shaped is ultimately derived and computationally compared with other models.

2 Shape optimization function definition for BSL

The effective performance of BSLs depends on the length of their ends and middle section. Hence, the main influential dimensions of BSLs includes the length of their ends (b) and middle section (a) considered as the design variables of optimization in this study (see Figure 1). In order to improve the energy dissipation and deformation ability of BSLs subjected to cyclic loading, maximizing the energy dissipated by plastic deformation (E_d) over the maximum equivalent plastic strain ($PEEQ_{\max}$) is adopted as the objective function of optimization. Therefore, the shape optimization problem of BSL is defined as indicated in Eq. (1).

$$\text{Find : } \mathbf{X} = \{a, b\}$$

$$\text{Maximize : } F(\mathbf{X}) = \frac{E_d}{PEEQ_{\max}} \quad (1)$$

The optimization function in Eq. (1) is considered to optimize the BSLs to have maximum energy dissipated energy capability before occurrence of any fracture in the system.

3 Grey Wolf Optimizer

Grey wolf optimizer (GWO) as a new meta-heuristic method was introduced by Mirjalili et al. [Mirjalili *et al.*, 2014]. The GWO algorithm based on using a new swarm intelligence algorithm was inspired by grey wolves. This algorithm simulates mimicking the hierarchical relationship and hunting behavior of grey wolves spontaneously. Hence, the GWO algorithm simulates the social hierarchy of grey wolves by the main four steps including social hierarchy, tracking, encircling, and attacking prey process. In GWO, the wolf hierarchy depicted in Figure 2 is simulated by four types of grey wolves: alpha (α), beta (β), delta (δ) and omega (ω).

The fittest solution is considered as α . Similarly, β and δ represents the second and third best solutions, respectively. ω is assumed as the last remaining best solutions. In the GWO algorithm, α , β , and δ wolves, respectively, guide the hunting (optimization), and the ω wolves follow these three wolves. As for encircling prey, the encircling prey mechanism is mathematically modelled in Eq. (2) and Eq. (3).

$$\mathbf{D} = |\mathbf{C} \cdot \mathbf{X}_p(l) - \mathbf{X}(l)| \quad (2)$$

$$\mathbf{X}(l+1) = \mathbf{X}(l) - \mathbf{A} \cdot \mathbf{D} \quad (3)$$

where \mathbf{X} and \mathbf{X}_p are the position vector of whales and prey at l th iteration, respectively; and \mathbf{A} and \mathbf{C} are respectively the coefficient vectors and emphasize exploitation and exploration, which can be obtained from Eq. (4) and Eq. (5).

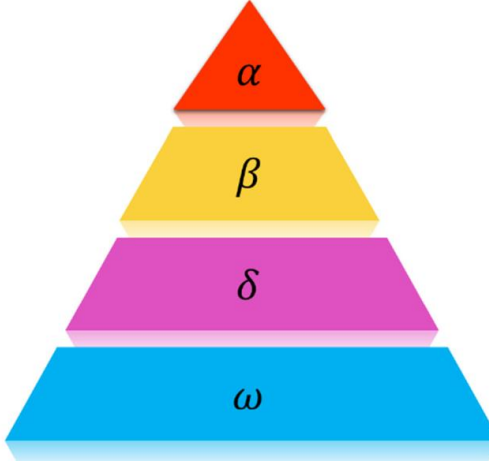


Figure 2 - *Hierarchy of grey wolf in GWO algorithm*

$$\mathbf{A} = 2\mathbf{a} \cdot \mathbf{r}_1 - \mathbf{a} \quad (4)$$

$$\mathbf{C} = 2\mathbf{r}_2 \quad (5)$$

where \mathbf{a} is linearly decreased from 2 to 0, \mathbf{r}_1 and \mathbf{r}_2 are random vectors between 0 and 1. Thus, \mathbf{A} is a random value in the interval $[-\mathbf{a}, \mathbf{a}]$. The vector \mathbf{C} can be regarded as the effect of obstacles close to prey in nature. The random values of \mathbf{C} provides random weights for the prey, which can avoid local optima stagnation, especially in the last iterations.

The position of prey and hunt are ordinarily guided by the α wolf and can be searched grey wolves. In each iteration, the α , β , and δ wolves can be obtained and oblige the other search agents (including the ω) to update their positions based on the current first three best positions. The process is formulated in Eqs. (6-8).

$$\mathbf{D}_i = |\mathbf{C}_j \cdot \mathbf{X}_i - \mathbf{X}| \quad (i = \alpha, \beta, \delta ; j = 1, 2, 3) \quad (6)$$

$$\mathbf{X}_j = \mathbf{X}_i - \mathbf{A}_j \cdot \mathbf{D}_i \quad (i = \alpha, \beta, \delta ; j = 1, 2, 3) \quad (7)$$

$$\mathbf{X}(l+1) = \frac{\mathbf{X}_1 + \mathbf{X}_2 + \mathbf{X}_3}{3} \quad (8)$$

4 Finite element modeling methodology for of butterfly-shaped links

4.1 FE modeling of BSL and plastic strain estimation

For the finite element (FE) analysis of BSLs in the optimization procedure, the FE modeling and validation of BSLs is explained in this section. The FE modeling and analysis of BSL were accomplished by a Python script in the FE package ABAQUS. For this purpose, the shell element (S4R), which is a 4-node with reduced integration and hourglass control, was used to simulate the behavior of BSL. The combined isotropic/kinematic hardening as constitutive law was selected to describe the material cyclic behavior. In the numerical material law, the nonlinear kinematic hardening component is obtained by superimposing two or more nonlinear kinematic hardening models which is summarized in Eq. (9).

$$\alpha = \sum_{k=1}^n \frac{C_k}{\gamma_k} (1 - e^{-\gamma_k \bar{\varepsilon}^{pl}}) \quad (9)$$

where n is the number of back-stresses. C and γ are the material parameters that are calibrated from cyclic test data. C is the initial kinematic hardening module, whereas γ determines the rate at which the kinematic hardening module decreases with increasing plastic deformation. $\bar{\varepsilon}^{pl}$ is equivalent plastic strain, called *PEEQ*.

The isotropic hardening component defines the evolution of the yield surface size, as a function of the equivalent plastic strain. This evolution is expressed by the simple exponential law shown in Eq. (10).

$$\sigma^0 = \sigma_0 + Q_\infty (1 - e^{-b \bar{\varepsilon}^{pl}}) \quad (10)$$

where σ^0 is the initial yield stress at zero plastic strain; Q_∞ and b are material parameters. Q_∞ is the maximum change in the size of the yield surface.

The total energy dissipation through plastic deformations, denoted by E_d , can be obtained from the ABAQUS output and is defined in Eq. (11).

$$E_d = \int_V \int_0^{\bar{t}} \sigma : \dot{\varepsilon}^{pl} dt dV \quad (11)$$

where σ and $\dot{\varepsilon}^{pl}$ are the stress tensor and the incremental plastic strains, respectively; V is the total volume of BSF; and \bar{t} is the duration of loading.

4.2 Verification of FE modeling methodology

The verification of FE modelling for BSF using ABAQUS software is implemented based on the laboratory test results. For this purpose, the specimen B10-36W tested by Ma et al. [Ma *et al.*, 2010] is chosen due to having both yielding and lateral torsional limit states occurred within the mode under cyclic loading (Figure 3(a)). In the FE modelling, the bottom edge of the plate is fixed, and the upper edge is tied to a reaction frame similar to corresponding test conditions. A displacement controlled loading history is applied at the top of the reaction frame, and for the fuses structure four nodded shell element with reduced integration (S4R) is used to avoid shear locking effects with five integration point through the thickness based on the previous studies recommendations which is shown in Figure 3.b [Farzampour *et al.*, 2015, Farzampour *et al.*, 2018]. The dynamic explicit solver is used to capture the pushover curves for the monotonic and cyclic behavior.

The cyclic loading condition is based on the AISC code loading for link to column connection, which is shown in Figure 4, and the monotonic loading is applied with in eight seconds from 0 up to 20% drift ratio of displacement-controlled loading.

A mesh sensitivity analysis was conducted resulting in approximately 10 mm element size (or less) in the shear plate. The possibility of shear locking and hour glassing effect is considered and avoided by choosing S4R element as the selected element type. The material constitutive model is specified with the coupon test results reported from the laboratory test. The material had a yield stress of 273 MPa, ultimate stress of 380 MPa, and linear kinematic hardening parameters are evaluated based on the given coupon test data [Ma *et al.*, 2010].

Based on Figure 5, the pushover results for monotonic and cyclic loadings are more 91% and 98% agreement with the experimental test pushover curves based on the comparison of the ultimate strength peaks captured in each cycle of loading.

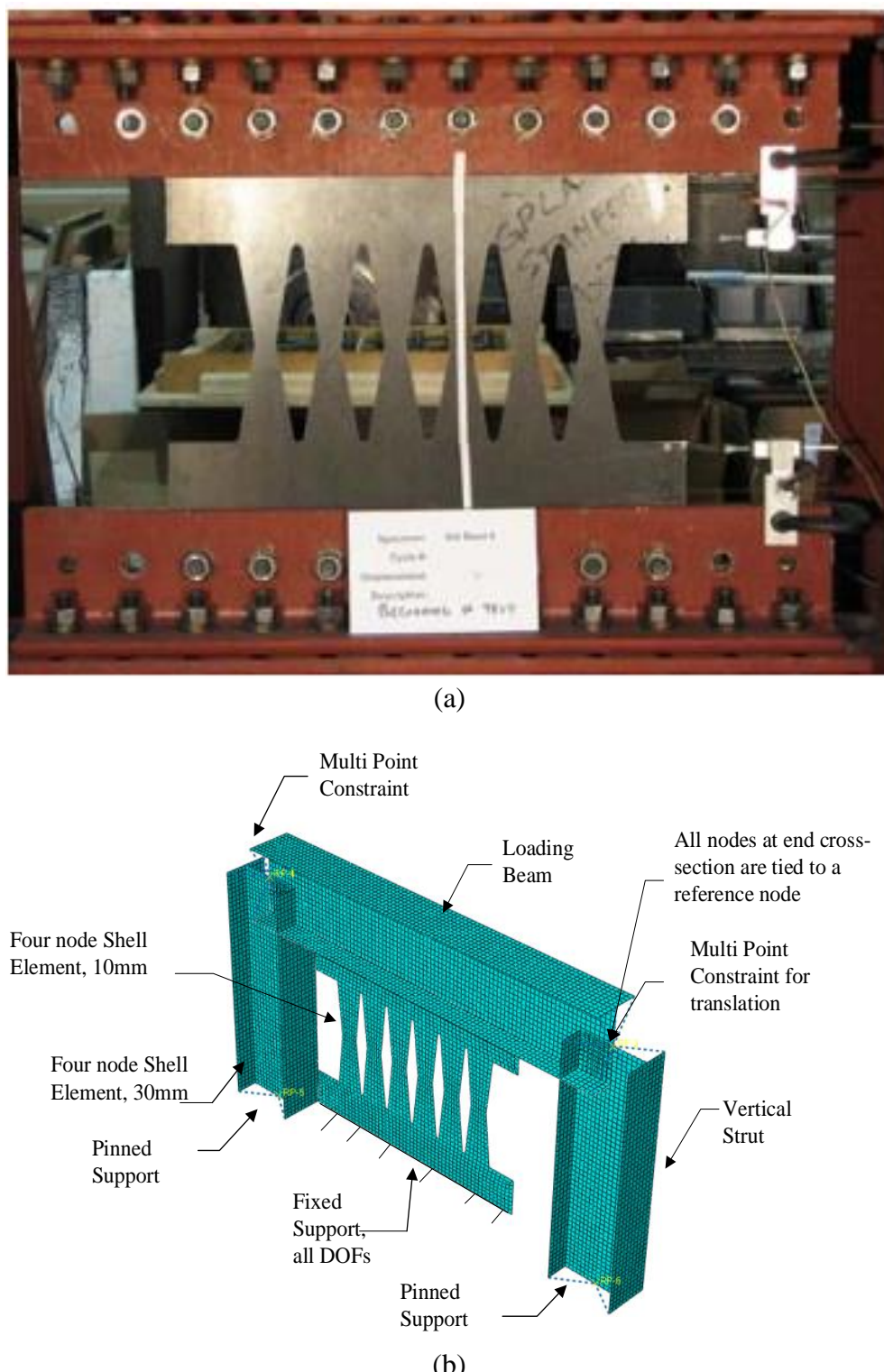


Figure 3 - (a) The model of laboratory test [Ma *et al.*, 2011], (b) The FE model of laboratory test simulated in ABAQUS

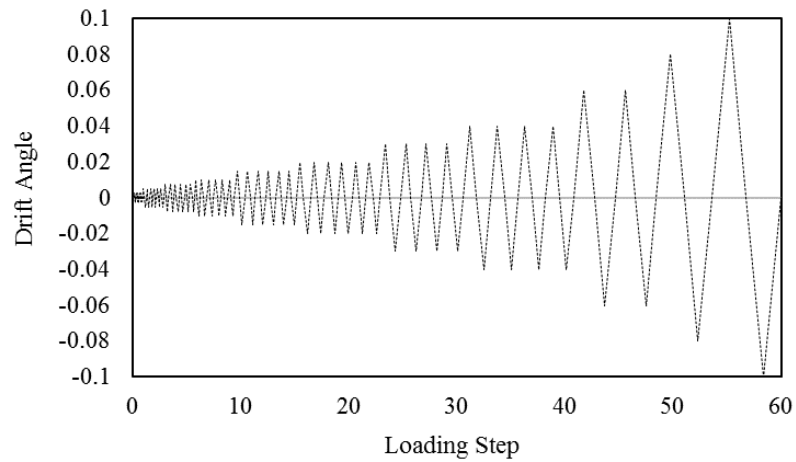


Figure 4 - The loading protocol for the verification of FE modeling

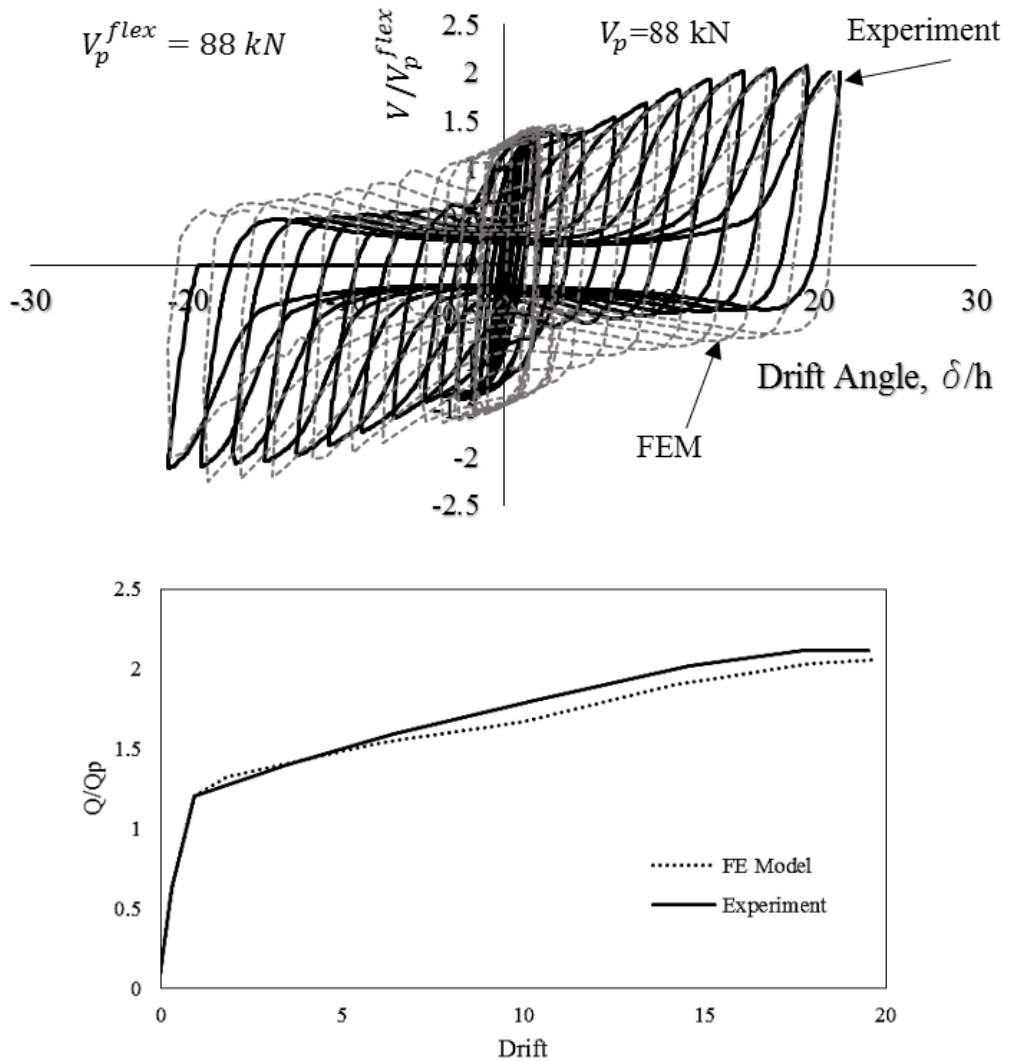


Figure 5 - Verification of modeling methodology under cyclic and monotonic loading

5 Description of the optimization results

In this section, with the aid of the finite element software package, a set of 300 iterations are considered for optimizing the limit state function elaborated in previous sections. The optimization process used about 72 hours of process with 40 CPUs. The nonlinear load-deformation behaviour and pushover behaviour of the structural shear links are investigated considering various geometrical shapes.

The geometrical parameters range included in optimization study are as follows. The length of the links, L , is set to be 0.5m for all the models. The slenderness ratio is selected to be carrying over of 10 to 50. The BSLs taper ratio (a/b) which typically controls the inelastic behavior of the link is varied over the range of 0.017 up to 3. In addition, the b/L ratio which takes values from the range of 0.2 up to 0.95 indicating as the major parameters for optimizing the link behavior. The essence of BSL optimization is to have energy dissipation capability in off concentrated plastic strain areas, which results in a more uniform stress distribution in larger drift values. Figure 6 shows the general schematic shape of BSL, the boundary condition at the bottom is fixed, and is restrained against out-of-plane vertical displacements at top. The Eigenvalue analysis is initially conducted for applying $L/250$ out-of-plane initial imperfection displacement based on the first buckling mode. Subsequently, the load is applied on the top edge of the link and pushover results are obtained and monitored at different drift values. It is noted that the load type is assumed to be displacement-control compatible with verified structural laboratory tests.

The material model has yield stress of 300 MPa, and ultimate stress of 345 MPa. The hardening is linear between the yielding point and ultimate point. The displacement control monotonic loading is applied at the top boundary of each model for extracting the pushover curve based on which the dissipated energy and maximum plastic strains are calculated. To achieve high precision the mesh sensitivity analysis is conducted to reach to the appropriate fine mesh size by having the results of push over and equivalent plastic strain converged. It is concluded that 5mm four nodded reduced order shell elements could be used for establishing the models to reduce the chance of shear locking and hour glassing effects. In addition, for having accuracy in finite element modelling, it is recommended to use at least 8 and 20, and 30 elements at the middle length (a), top length (b) and inclined length of BSLs.

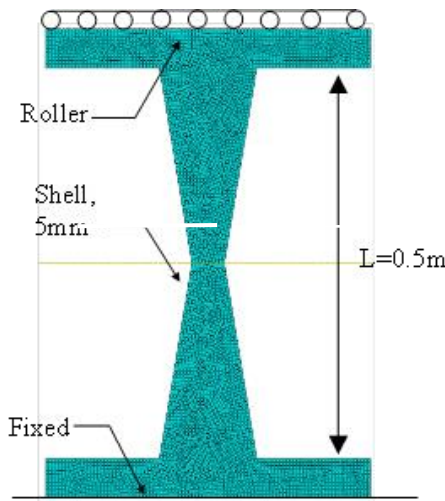


Figure 6 - The schematic geometrical properties of a typical BSL

The optimization procedure is conducted by a system integrating of MATLAB and ABAQUS software packages for analysis purposes. The iteration process is illustrated in Figure 7. At the initial stage, ABAQUS reads the python script and run the analysis job. Then the results based on the optimization function is estimated and transferred to MATLAB to analyze the results with the aid of GWO algorithms and update the variables. From this step, a new model is produced by Python script for the next iteration. As the iteration number goes higher, the models will approach to the optimal function value. It is noted that the implementation of the Python scrip allows the finite element analysis and GWO algorithm to be combined and conjugated.

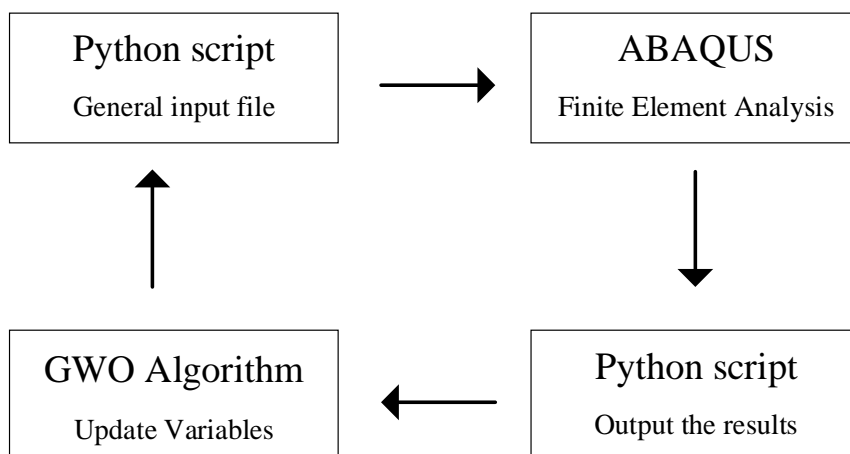


Figure 7 - Optimization flow chart based on which the optimization criterion works

The distribution of the plastic strain is indicated in Figure 8 for a handful general BSLs models at the 5% drift ratio. The optimized model based on the proposed criterion is compared with other FE simulated BSL's which is shown in Figure 8. In order to optimize the model for having maximum energy dissipation capability with less potential for fracture, the GWO algorithms are implemented to generate the optimization function. The optimized models are subjected to loading condition described previously. After implementation of the GWO algorithms, the plastic strain values are decreased by 51 percentage at 5% drift ratio compared to the average values of the plastic strains. This would indicate that the optimal model is able to avoid fracture and accumulation of plastic strains leading to capability of resisting towards loads in larger drift values. In addition, as it shown in Figure 8.d, the optimal models is able to concentrate the plastic strain far from the sharp angle and geometrical changes which indicates better capability in avoiding the fractures. The distribution of plastic strain concentration within the models is shown to be consistently uniform for optimal model compared to the rest. This observation will indicate that the proposed optimization methodology allows more energy dissipation far from the sharper angles at points in which the concentration of the strains might occur under the applied loading. From the plastic strain investigation of the models with optimized model, it is concluded that the behavior of the models are generally categorized into four different groups concerning plastic strain accumulation. First, the straight models shown in Figure 8a would generally concentrate the plastic strain values at the ends of BSLs, these models have highest PEEQ values at the same drift compared to the rest of BSLs. Second, the models shown in Figure 8.b that concentrate the plastic strains at the middle, which is the place where the shear yielding occurs [Farzampour and Eatherton, 2018a, 2018b]. Third, the models

shown in Figure 8.c in which the buckling limit state occurs, hence the model would not be able to dissipate energy as it loses the capability of load bearing resistance in medium to large drifts. Fourth, the optimal type models shown in Figure 8.d in which the flexural and shear yielding occur simultaneously without any brittle limit state observed. This model is able to dissipate energy without occurrence of fracture; hence, maximizing the optimizing the limit state function. Along the same lines, Figure 9 shows the stress distribution of the selected models after experiencing five percent drift ratio. It is concluded that the stress distribution of the optimal model has more uniform distribution along the length of the links, proposing better implementation of material, and higher energy dissipation values. It is noted that the optimal model geometrical properties based on the transitions equation provided by Farzampour and Eatherton [Farzampour and Eatherton, 2018a, 2018b] determines that the model is at the stage of behavioral mode change from flexure yielding to shear yielding. In addition, from the optimization analysis, it is concluded that those models that have thicker plates have better capability in maximizing the optimizing function due to better resistance against buckling as it is indicated in Eq. (1). It is noted that the optimal model has better ability to distribute stress over the length of the link, while other models concentrate the stresses in specific parts as it is illustrated in Figure 9.

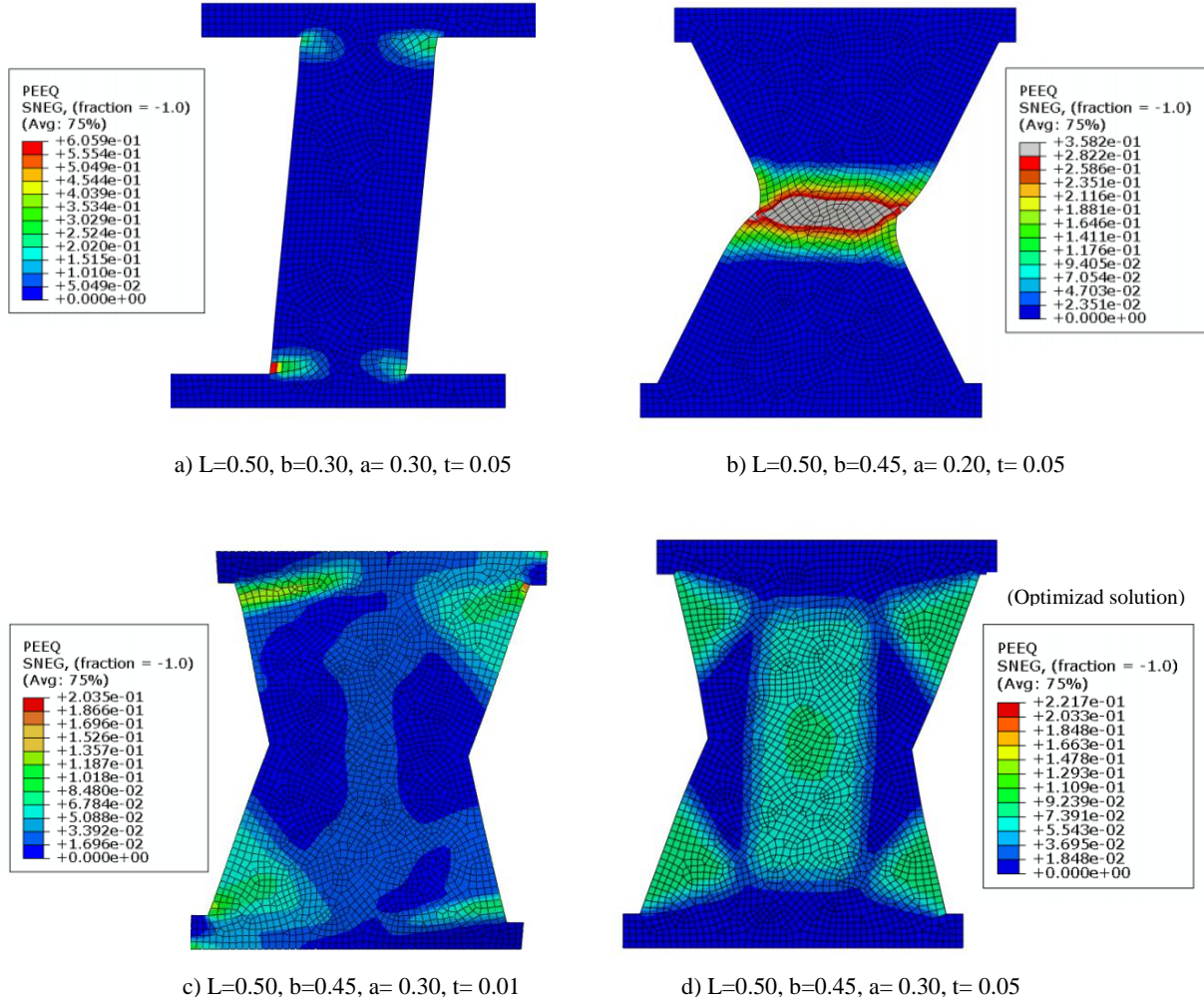
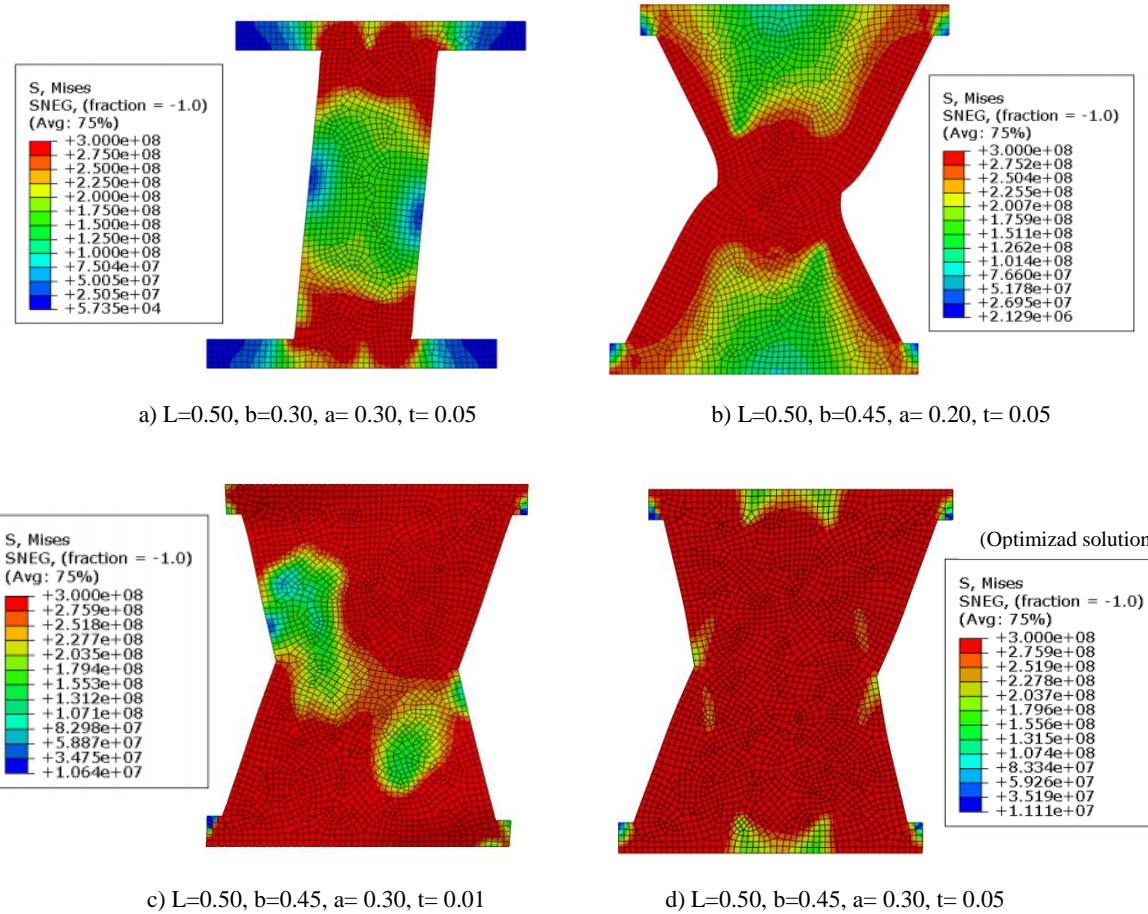


Figure 8 - Plastic strain accumulation of BSF fuses

Figure 9 - *von-Mises stress distribution for BSL fuses*

Hence, less possibility of fracture is expected for the optimal BSL model. The optimal model also demonstrates improved energy dissipation capacity compared to the rest of the corresponding BSL models.

In order to have a better behavioral comparison between different models, the results of normalized maximum PEEQ, normalized dissipated energy and optimization function are summarized in Table 1. The normalization is done based on the values associated with optimal solution. It is noted that the maximum PEEQ value for optimal model at 5% drift value is 0.221, and the dissipate energy is 656.22 kN m. It is concluded that the buckling resistant models can dissipate energy more effectively if they are designed in such way that flexure and shear yielding limit states occur simultaneously to distribute the plastic strains and stresses along the length of the link.

6 Conclusions

In this study, after validation of finite element methodology, over 300 butterfly shaped links are generated. The optimization criterion function is introduced to evaluate the dissipated energy over the concentrated PEEQ values to find the optimized geometrical properties for a typical butterfly-shaped link. Subsequently, Grey Wolf Optimizer algorithms are used to maximize dissipation energy capability and reduce concentration of plastic strains for butterfly-shaped links. Based on the proposed method, optimal values occur for a geometry in which the

flexural yielding mode transforms to shear yielding point. For a link with 0.5m length, the mid-width of 0.3m, end width of 0.45, and thickness of 0.05 are obtained as the optimal shape for the butterfly-shaped link. This observation will indicate that the optimization methodology proposed in this study results in generation of models with appropriate energy dissipation features and less potential for fracture. It is shown that for the optimal model, the plastic strain concentration points are developed far from the sharper geometrical changes, causing a better resistance against possible fractures.

Table 1 - *Sample of the results for optimization study on BSLs*

No.	<i>L</i>	<i>t</i>	<i>b</i>	<i>a</i>	Normalized PEEQ ^{max}	Normalized <i>E_d</i>	<i>E_d</i> /[PEEQ ^{Max}]
1	0.5	0.01	0.1	0.008	2.3	0.002	494
2	0.5	0.01	0.1	0.154	1.6	0.029	11,984
3	0.5	0.01	0.1	0.3	1.3	0.034	17,169
4	0.5	0.01	0.275	0.154	1.8	0.088	31,882
5	0.5	0.01	0.275	0.3	2.4	0.098	27,211
6	0.5	0.01	0.45	0.008	1.0	0.033	21,394
7	0.5	0.01	0.45	0.154	1.6	0.098	41,586
8	0.5	0.01	0.45	0.3	1.1	0.174	107,723
9	0.5	0.03	0.1	0.008	2.3	0.005	1,505
10	0.5	0.03	0.1	0.154	1.6	0.086	35,873
11	0.5	0.03	0.1	0.3	1.3	0.104	52,633
12	0.5	0.03	0.275	0.008	1.9	0.057	19,529
13	0.5	0.03	0.275	0.154	1.5	0.057	24,982
14	0.5	0.03	0.275	0.3	2.3	0.310	86,847
15	0.5	0.03	0.45	0.008	1.0	0.100	64,588
16	0.5	0.03	0.45	0.154	1.5	0.297	125,903
17	0.5	0.03	0.45	0.3	1.0	0.600	386,997
18	0.5	0.05	0.1	0.008	2.3	0.009	2,512
19	0.5	0.05	0.1	0.154	1.6	0.144	59,808
20	0.5	0.05	0.1	0.3	1.3	0.173	87,867
21	0.5	0.05	0.275	0.008	1.9	0.095	32,502
22	0.5	0.05	0.275	0.154	1.5	0.448	190,310
23	0.5	0.05	0.275	0.3	2.3	0.517	145,639
24	0.5	0.05	0.45	0.008	1.0	0.167	107,627
25	0.5	0.05	0.45	0.154	1.5	0.495	209,882
26	0.5	0.05	0.45	0.3	1.0	1.000	656,248
27	0.5	0.05	0.47	0.35	1.7	0.932	353,779
28	0.5	0.05	0.418	0.3	1.0	0.878	599,929

References

- Castaldo, P., Palazzo, B. and Perri, F. (2016). Fem simulations of a new hysteretic damper: The dissipative column. Ingegneria Sismica, **33**(1), 34-45.
- Deng, K., Pan, P., Sun, J., Liu, J. and Xue, Y. (2014). Shape optimization design of steel shear panel dampers. Journal of Constructional Steel Research, **99**, 187-193.

- Farzampour, A. (2019). *Evaluating Shear links for Use in Seismic Structural Fuses*. Doctoral dissertation, Virginia Tech, United States.
- Farzampour, A. and Eatherton, M.R. (2017). Lateral torsional buckling of butterfly-shaped shear links, Proc. of the SSRC Annual Stability Conference Structural Stability Research Council, San Antonio, USA.
- Farzampour, A. and Eatherton, M.R. (2018a). Investigating limit states for butterfly-shaped and straight shear links, Proc. of the 16th European Conference on Earthquake Engineering, 16ECEE, Thessaloniki, Greece.
- Farzampour, A. and Eatherton, M.R. (2018b). Parametric study on butterfly-shaped shear links with various geometries, Proc. of the 11th National Conference on Earthquake Engineering, 11NCEE, Los Angeles, USA.
- Farzampour, A. and Eatherton, M.R. (2019). Yielding and lateral torsional buckling limit states for butterfly-shaped shear links. *Engineering Structures*, **180**, 442-451.
- Farzampour, A., Laman, J.A. and Mofid, M. (2015). Behavior prediction of corrugated steel plate shear walls with openings. *Journal of Constructional Steel Research*, **114**, 258-268.
- Farzampour, A., Mansouri, I., Lee, C.H., Sim, H.B. and Hu, J.W. (2018). Analysis and design recommendations for corrugated steel plate shear walls with a reduced beam section. *Thin-Walled Structures*, **132**, 658-666.
- Hitaka, T. and Matsui, C. (2003). Experimental study on steel shear wall with slits. *Journal of Structural Engineering*, **129**(5), 586-595.
- Jiménez-Alonso, J.F. and Sáez, A. (2017). Robust optimum design of tuned mass dampers to mitigate pedestrian-induced vibrations using multi-objective genetic algorithms. *Structural Engineering International*, **27**(4), 492-501.
- Khatibinia, M. and Sadegh Naseralavi, S. (2014). Truss optimization on shape and sizing with frequency constraints based on orthogonal multi-gravitational search algorithm. *Journal of Sound and Vibration*, **333**(24), 6349-6369.
- Lee, C.H., Ju, Y.K., Min, J.K., Lho, S.H. and Kim, S.D. (2015a). Non-uniform steel strip dampers subjected to cyclic loadings. *Engineering Structures*, **99**, 192-204.
- Lee, C.H., Kim, J., Kim, D.H., Ryu, J. and Ju, Y.K. (2016a). Numerical and experimental analysis of combined behavior of shear-type friction damper and non-uniform strip damper for multi-level seismic protection. *Engineering Structures*, **114**, 75-92.
- Lee, C.H., Lho, S.H., Kim, D.H., Oh, J. and Ju, Y.K. (2016b). Hourglass-shaped strip damper subjected to monotonic and cyclic loadings. *Engineering Structures*, **119**, 122-134.
- Lee, C.H., Woo, S.-K., Ju, Y.K., Lee, D.-W. and Kim, S.-D. (2015b). Modified Fatigue Model for Hourglass-Shaped Steel Strip Damper Subjected to Cyclic Loadings. *Journal of Structural Engineering*, **141**(8), 04014206.
- Liu, T., Zhang, Q., Zordan, T. and Briseghella, B. (2016). Finite element model updating of canonica bridge using experimental modal data and genetic algorithm. *Structural Engineering International*, **26**(1), 27-36.
- Longo, A., Montuori, R. and Piluso, V. (2016). Moment frames – concentrically braced frames dual systems: analysis of different design criteria. *Structure and Infrastructure Engineering*, **12**(1), 122-141.

- Luth, G., Krawinkler, H. and McDonald, B. (2008). USC School of Cinema: An example of repairable performance based design, Proc. of the 77th Annual Structural Engineers Association of California (SEAOC) Convention, Structural Engineers Association of Southern California, Fullerton, CA.
- Ma, X., Borchers, E., Peña, A., Krawinkler, H., Billington, S. and Deierlein, G. (2010), "Design and behavior of steel shear plates with openings as energy-dissipating fuses", Report No. 173, The John A. Blume Earthquake Engineering Center, Stanford University, USA.
- Mansouri, I., Hu, J.W. and Kişi, O. (2016). Novel predictive model of the debonding strength for masonry members retrofitted with FRP. *Applied Sciences* (Switzerland), **6**(11).
- Martínez-Rueda, J.E. (2002). On the evolution of energy dissipation devices for seismic design. *Earthquake Spectra*, **18**(2), 309-346.
- Mirjalili, S., Mirjalili, S.M. and Lewis, A. (2014). Grey Wolf Optimizer. *Advances in Engineering Software*, **69**, 46-61.
- Mirzai, N.M., Attarnejad, R. and Hu, J.W. (2018). Enhancing the seismic performance of EBFs with vertical shear link using a new self-centering damper. *Ingegneria Sismica*, **35**(4), 57-76.
- Mirzai, N.M., Zahrai, S.M. and Bozorgi, F. (2017). Proposing optimum parameters of TMDs using GSA and PSO algorithms for drift reduction and uniformity. *Structural Engineering and Mechanics*, **63**(2), 147-160.
- Montuori, R., Nastri, E. and Piluso, V. (2016). Preliminary analysis on the influence of the link configuration on seismic performances of MRF-EBF dual systems designed by TPMC. *Ingegneria Sismica*, **33**(3), 52-64.
- Montuori, R., Nastri, E. and Piluso, V. (2017a). Influence of the bracing scheme on seismic performances of MRF-EBF dual systems. *Journal of Constructional Steel Research*, **132**, 179-190.
- Montuori, R., Nastri, E., Piluso, V. and Troisi, M. (2017b). Influence of connection typology on seismic response of MR-Frames with and without 'set-backs'. *Earthquake Engineering and Structural Dynamics*, **46**(1), 5-25.
- Mukhopadhyay, T., Dey, T.K., Dey, S. and Chakrabarti, A. (2015). Optimisation of fibre-reinforced polymer web core bridge deck - A hybrid approach. *Structural Engineering International*, **25**(2), 173-183.
- Nastri, E., Montuori, R. and Piluso, V. (2015). Seismic design of MRF-EBF dual systems with vertical links: EC8 vs plastic design. *Journal of Earthquake Engineering*, **19**(3), 480-504.
- Okasha, N.M. (2016). System reliability based multi-objective design optimization of bridges. *Structural Engineering International*, **26**(4), 324-332.
- Salajegheh, E., Gholizadeh, S. and Khatibinia, M. (2008). Optimal design of structures for earthquake loads by a hybrid RBF-BPSO method. *Earthquake Engineering and Engineering Vibration*, **7**(1), 13-24.
- Teruna, D.R., Majid, T.A. and Budiono, B. (2015). Experimental study of hysteretic steel damper for energy dissipation capacity. *Advances in Civil Engineering*, **2015**, 1-12.
- Whittaker, A.S., Bertero, V.V., Thompson, C.L. and Alonso, L.J. (1991). Seismic testing of steel plate energy dissipation devices. *Earthquake Spectra*, **7**(4), 563-604.
- Zeynali, K., Saeed Monir, H., Mirzai, N.M. and Hu, J.W. (2018). Experimental and numerical investigation of lead-rubber dampers in chevron concentrically braced frames. *Archives of Civil and Mechanical Engineering*, **18**(1), 162-178.
- Zhu, B., Wang, T. and Zhang, L. (2018). Quasi-static test of assembled steel shear panel dampers with optimized shapes. *Engineering Structures*, **172**, 346-357.



OTTIMIZZAZIONE DELLA FORMA DI LINK A TAGLIO REALIZZATI CON ELEMENTI A PLASTICITÀ DIFFUSA MEDIANTE UN ALGORITMO DEL TIPO GREY WOLF.

Alireza Farzampour¹, Mohsen Khatibinia², Iman Mansouri³

¹Department of Civil and Environmental Engineering, Virginia Tech, United States

²Department of Civil Engineering, University of Birjand, Birjand, Iran

³Department of Civil Engineering, Birjand University of Technology, P.O. Box 97175-569,
Birjand, Iran

SOMMARIO: *Il carico di taglio applicato alle strutture è contrastato dall'implementazione di dissipatori isterici come sistema di resistenza sismica strutturale. Recentemente, sono state introdotte piastre in acciaio con intagli progettati per avere una risposta controllata. Questi elementi strutturali che si comportano come i link a taglio sono in grado ritardare forme di collasso fragili. Tra questi, un tipo di collegamento molto promettente è il cosiddetto collegamento a forma di farfalla, per il quale il diagramma del momento richiesto si allinea al diagramma del momento ottenuto. Studi precedenti mostrano che questi elementi sono usati come scelta appropriata per il sistema di fusibili sismici poiché sono in grado di sperimentare grandi escursioni in campo plastico con duttilità sufficiente e comportamento isterico completo. Pertanto, le proprietà geometriche appropriate per questi collegamenti necessitano di ulteriori indagini. In questo studio, la metodologia degli elementi finiti è inizialmente validata con test sperimentali. Quindi vengono introdotti criteri di ottimizzazione per un set di 300 modelli per studiare le proprietà geometriche desiderate per avere la maggior parte della dissipazione di energia con un minor potenziale di frattura. Questo lavoro propone il processo di ottimizzazione con il quale le proprietà geometriche del dispositivo a forma di farfalla sono state migliorate per avere prestazioni di dissipazione dell'energia sufficienti e minor potenziale di frattura. Le curve di pushover e le deformazioni plastiche equivalenti sono ottenute da ABAQUS attraverso un processo iterativo. Il metodo di ottimizzazione "Grey Wolf" è stato adottato grazie all'elevata capacità nell'ambito di sistemi non lineari. Si può scoprire che mediante l'implementazione del metodo di ottimizzazione i link sono progettati per avere un cambio di modalità di rottura dalla flessione al taglio e sono in grado di dissipare energia su un valore di deformazione plastica minore.*

PAROLE CHIAVE: *Fusibili sismici strutturali, "Grey Wolf", Link a forma di farfalla, Elementi finiti, Deformazioni plastiche*